Landslide Susceptibility Assessment using GIS-based multicriteria Decision Analysis (MCDA) along a part of National Highway-1, Kashmir- Himalayas, India

Iftikhar Hussain Beigh

iftikharbeigh@nitsri.ac.in

National Institute of Technology Srinagar,Jammu and Kashmir,India

Kaiser Bukhari

National Institute of Technology Srinagar, Jammu and Kashmir, india

Research Article

Keywords: Analytic hierarchy process (AHP), Landslide susceptibility, Kashmir Himalaya, National Highway-1(NH-1), MCDA, Geographic Information System (GIS)

Posted Date: November 8th, 2023

DOI: https://doi.org/10.21203/rs.3.rs-3347229/v1

Version of Record: A version of this preprint was published at Applied Geomatics on March 26th, 2024.
See the published version at https://doi.org/10.1007/s12518-024-00559-6.

Landslide Susceptibility Assessment using GIS-based Multicriteria Decision Analysis (MCDA) along a part of National Highway-1, Kashmir- Himalayas, India.

Iftikhar Hussain Beigh and Kaiser Bukhari

Department of Civil Engineering National Institute of Technology Srinagar-190006, India
Corresponding Email: iftikharbeigh@nitsri.ac.in

Abstract

The current study aims at GIS-based multicriteria decision analysis (AHP) to generate a landslide-susceptible map from Baramulla to Uri Road segment along NH-1, Kashmir Himalaya, India. The landslide causative factors examined to generate our AHP matrix are slope gradient, elevation, slope aspect, curvature, distance to drainage, distance to roads, distance to lineaments, geology, land use land cover (LULC), and Rainfall. The study mapped and identified the active landslides along NH-1 through extensive field investigations and other secondary data sources. The landslide events were dominated by rockfall and debris slides. Based on their importance in landslide occurrences, the thematic layers were given relative relevance scores using Saaty's scale. Besides, the Analytic Hierarchy Process (AHP) was employed to normalize the relative weights and attributes of the various thematic layers. In addition, all thematic data layers were combined using a weighted linear approach to generate the landslide susceptibility (LS) map. Furthermore, the resultant LS map was classed into five categories viz., very high (24.18 %), high (30.24%), medium (28.61%), low (15.28%), and very low (1.69 %). The study reveals that 54.42 % of the area falls under the high and very high susceptible zones. Likewise, 78.9% of overall model accuracy was computed from the Area under curve (AUC) method. Moreover, this study would aid infrastructural, geo-environmental, and landslide hazard planning in the studied region.

Keywords Analytic hierarchy process (AHP) · Landslide susceptibility · Kashmir Himalaya · National Highway-1(NH-1) · MCDA · Geographic Information System (GIS).

Introduction

Landslides concern people worldwide (NDMA 2009). The movement of substantial quantities of rock, earth, or debris down a slope is called a landslide (Cruden 1991). Globally, landslides rank third among natural disasters (Castellanos Abella 2008). Landslides affect most of India, especially the Himalayas and other hilly regions. Landslides can cause loss of human life, animal life, infrastructure, and area finances. The Indian Himalayan Region (IHR) is home to one of the world's most complex mountain ranges and one of the youngest mountain chains. More than 2400 kilometers of length is to the east, while its width ranges from 220 to 330 kilometers (Agarwal et al. 1997). The Himalayas' complex geo-tectonic structure, topography, and climate cause frequent landslides (Sangra et al. 2017, Singh et al. 2014). Due to increased social and economic awareness and human settlement in mountainous areas,

landslides have gained global attention (Aleotti and Chowdhury 1999). Heavy rain, earthquakes, water level changes, snowmelt, typhoons, etc. can cause landslides (Keefer 1984; Xie et al. 2015; Yang et al. 2016).

Several studies conducted in the Himalayas have mapped landslide hazards (Jamir et al. 2019; Pham et al. 2016; Mathew et al. 2009; Kamp et al. 2008; NRSA 2001). It has been noted by Dikshit et al. (2020) that landslide research is lacking in the North-Western Himalayas, particularly in Jammu and Kashmir. Research on landslides in this region is limited (Owen et al. 2008; Khattak et al. 2010; Mohammady et al. 2012; Chingkhei et al. 2013; Bilham and Bali 2014; Singh et al. 2014; Hussain et al. 2015; Singh and Som 2016; Sangra et al. 2017; Hussain et al. 2018; Nanda et al. 2020a.b; Bashir and Ramkumar 2021; Abhijit et al. 2021; Mohsin et al. 2022). In the Kashmir Himalaya, roads are crucial for socioeconomic development. In hilly areas like the Kashmir Himalayas, landslides and slope failures are common. In hilly areas, landslides are the most destructive. Traffic congestion caused by highway slope failures inconveniences passengers. Landslides can cause fatalities and financial losses. Construction of roads in hilly areas accelerates cutting-caused slope failure (Singh and Kumar 2018). Hence, highway construction disturbs natural slopes, increasing their failure risk. Assessing landslide risks along roadways is essential for the successful development and management of infrastructure (Singh and Kumar 2018). Landslide maps are used for both planning and mitigation. A landslide hazard map depicts locations susceptible to landslides. Studies of landslide hazards necessitate knowledge of the factors that activate landslides (Singh and Kumar 2018). The likeliness and severity of landslide disasters are amplified by factors like earthquakes, rainfall, erosion, etc. (Tanyas et al. 2019). Geographic information systems (GIS) manage spatial and temporal data effectively. It allows flexible input-to-output changes. Researchers use GIS to map landslide hazards and susceptibility (Fan et al. 2017; Singh and Kumar 2018). In GIS landslide mapping is performed using qualitative, quantitative, and semi-quantitative approaches (Shano et al. 2020). Quantitative approaches use mathematical estimates, while qualitative approaches are descriptive (Reichnenbach et al. 2018). Quantitative procedures are more precise than qualitative approaches, but they rely on an accurate inventory of landslides to be effective. Semi-quantitative or semi-qualitative approaches are hybrids. Semi-qualitative techniques include AHP, ANP, fuzzy-AHP, etc. (Chaiyaphan et al. 2020). Additionally, MCDA techniques are often used to combine environmental, socioeconomic, and technical criteria to make suitable decisions about any spatial challenge on Earth (Mohebbi et al. 2013). MCDA is an evaluation method that facilitates the ranking of several likely solutions by identifying assessment criteria with competing objectives (Balew et al. 2020). MCDA is comprised of numerous ways for evaluating spatial difficulty; nonetheless, AHP and WLC techniques are commonly employed for numerous suitability analyses. AHP solves complex problems into simple criteria, which are then weighted (Saaty 1980; Saaty 1987). Researchers have used AHP to map landslide hazards (Kumar and Anbalagan 2016). AHP helps find reliable solutions (Saaty 1980; Saaty 1987).

The study area selected is NH-1 from Baramulla to Uri, Kashmir Himalaya, India. NH-1 which runs near the Pakistan-India border in the Kashmir Himalayas, is strategically an important lifeline for the socioeconomic development of the region. Heavy rain or snow often triggers landslides on the highway. Landslides often damage the route and even road widening will make the situation worse. The present study area was chosen because it is among the most landslide potential areas in the Kashmir Himalaya. In addition, landslide occurrence in this region is mostly undocumented. Therefore, the current study is aimed at identifying the landslide-susceptible zones along NH-1 from

Baramulla to Uri Road in the Kashmir Himalayas, India using Gis-based MCDA (AHP) approaches. Furthermore, the scope of this research can be extended to investigate landslides in other regions of the Northwestern Himalaya, particularly Kashmir Himalaya. This study also emphasizes the need for landslide early warning systems (LEWS) and slope stability measures to reduce future landslides.

Study region

The present study area selected is situated between the Baramulla and Uri towns along the National Highway 1 (NH-1), North Kashmir Himalayas, India. Geographically it is extended between the Latitudes 34°1'35.38"N - 34°15'20.942"N and Longitudes 73°57'41.4"E - 74°24'10.11" E (Fig. 1). The study was conducted on a 45.0 km road stretch that travels along picturesque cliffs and mountainsides covered with trees. It encompasses Survey of India (SOI) toposheet No. 43J/4, 43J/8, and 43F/16, covering an area of 479.81 km^2. Due to the increasing population trend and the rapid urbanization in the hilly terrains, the slopes here are at high risk. NH-1 is the lifeline and one of the strategically essential roads of Kashmir Himalaya. Due to reoccurring slope failures NH- 1, along with the other roads, is badly affected, and the area suffers vast economic losses, especially during the bad weather. Tourism, which is a good source of economy, is usually hampered due to road failure, especially during the monsoon period. Also, agricultural products are badly affected by landslides. The region's climate is broadly Mediterranean continental, which features chilly, wet winters and cool, dry summers. From December to May, the region experiences its highest levels of snowfall and Rainfall, and from June to September, its lowest levels. The maximum slope failure incidents are reported during this time of the year. The area also lies in seismic zone V; incidents like earthquakes and landslides are widespread. The elevation ranges from 1098 to 3475 m above sea level. It has a rough, undulating topography. Downstream from the main town of Baramulla, most of the route follows the south banks of the Jhelum River. Baramulla, Khanpora, Sheeri, Gantamulla, Mahura, Lagama, and Uri are well-known locations along the road. The magnificent view of the mighty Pir Panjal range, which rises to an average elevation of 1400 m to 4,100 m above mean sea level (m amsl), can be found on the road's southern side. Due to vegetation and human settlements, tracing geology and soil continuity over great distances is impossible.

The soil of the research region is comprised of four primary groups: fine loamy (41.2%), coarse loamy (44.8%), calcareous loamy (0.1%), and fine silty soils (13.9%). The geological formations are as old as the Proterozoic age, characterized by salkhala formations (carbonaceous phyllite, schist, limestone, and dolomite), and as young as Eocene – Miocene age which is characterized by lower Murree formations (Shale, Sandstone, and Siltstone). Alluvium, moraines, hill wash, and scree make up 22.2% of the lithology of the study region, followed by phyllite, quartzite, diamictite, and lava flows (19.8 %). Extensively dissected hills and valleys constitute the majority of the study area's geomorphology (78.5%). Mild erosion, heavy precipitation, snowfall, weathering, tectonic activity, and other anthropogenic activities including road widening and an inadequate drainage system all contributed to slope collapse along the section of road under study.

Historical Landslide data

A study area's hillside, drainage, and steep slopes are found to be the most favorable sites for landslide activity. Earthquakes, heavy rain, and snow usually cause large and small landslides. However, some landslides have been reported to have been caused by human activities. A historical landslide database was compiled from various

governmental and non-governmental agencies, national and local newspapers, past research literature, and extensive frequent field visits. The current study shows major historical landslide events and their associated impacts as shown in Table 1. During fieldwork, it was observed that human activities such as haphazard hillside development, road widening, and inappropriate drainage embankment construction along the slope are responsible for triggering landslides. In addition, throughout the field visit, not all landslide events were documented if they did not injure or damage Construction (buildings, roads, etc.).

Materials and methods

The precision of the LSZ map is dependent on the selection and quality of the landslide inventory as well as the elements that increase the likelihood of landslides occurring (Bathrellos et al. 2012). Likewise, a landslide inventory database keeps track of where landslides are, what kind they are, how big they are, and what caused them (Lageson et al.2016). The scope and readiness of the data, as well as the time frame and cost of the project, affect how the predisposing factors are chosen (Chen et al. 2014). For this study, 109 landslide locations, which occurred from 1990-2022, were used along with 10 casual factors for the landslide susceptibility assessment.

Landslide Inventory Mapping and Landslide Mechanism

The investigation of the potential for landslides always begins with the compilation of a detailed inventory (Pradhan- et al. 2010). Location, landslide type, activity, and physical details are all included in the inventory (Fell et al. 2008). Considering the same conditions that led to previous landslides is a common starting point for landslide hazard modeling (Dagdelenler et al. 2016). Therefore, the preparation of a comprehensive landslide inventory map is crucial. Mapping prior landslides helps to understand their causes and parameters (Guzzetti et al. 1999) and validate the final LHZ map.

A comprehensive landslide inventory was prepared with the aid of both primary (extensive field surveys during 2019-2021) and secondary sources (historical material from newspapers, local interviews, Government departments like Border Road Organization (BRO), Geological Survey of India (GSI), and Roads and Buildings Department(R&B). It should be noted that the inventoried landslides did not necessarily occur in a single episode, but rather, in several instances, the landslides followed a sequential pattern, with numerous tiny landslides occurring in the same region, close together.

During a field survey, handheld GPS, measuring tape, and Brunton compass were employed to verify and update the information. The study area had 109 minor and major landslides (Fig. 2). The landslide inventory mapping data for model validation were divided into Training Samples (70%) and Tested Samples (30 %). Rockfalls and Debris slides were found to be the predominant types of landslides. The landslides were categorized by using Cruden and Vandine (2013) and Cruden and Varnes (1996) developed landslide classification scheme and are well depicted in Fig. 3. Furthermore, debris slide was revealed to be the predominant type (54 %) of landslide movement, followed by rockfall type (32 %) (Fig.3a-d). Most of the landslide activity observed (68 %) was of the active type. The landslide activity distribution was dominated by the widening type (29%), followed by the advancing type (24%) (Fig.3c). The most common style of landslide activity type was found to be multiple types (71%), followed by single type (22%) (Fig.3d).

According to the Literature review and fieldwork, hill cutting in the study region triggers landslides. Hills are frequently cut at their base to make place for highways, tunnels, and trains, for extraction purposes, or simply to make room for the construction of new and non-manufactured huts (prepared of poor waste materials and wood). This raises the steepness of the slope, which reduces its stability. Consequently, this strategy will put lives and property at landslide risk. Moreover, other triggers of landslide occurrences are adversely oriented structural discontinuity, weak and weathered materials, contrast in permeability, deforestation, incessant precipitation (rainfall), slope or its toe excavation, improper drainage, and irrigation.

Thematic Layer Preparation

Ten thematic maps were prepared in RS and GIS platforms to prepare a final LSZ map. These thematic layers include slope gradient, elevation, slope aspect, slope curvature, distance to drainage, geology, distance to lineaments, land use/landcover, distance to roads, and precipitation (Rainfall). The lineaments were extracted from high-resolution satellite imagery motivated by the National Remote Sensing Centre (NRSC) Bhuvan, supporting lineament data. Using maximum likelihood classification and ground control points, a LULC map was generated using Landsat 8 OLI data. The topographic parameters like Slope gradient, elevation, slope aspect, slope curvature, and hydrological parameter (drainage) were generated from ALOS PALASAR-DEM. A Euclidean distance approach (proximity analysis tool) in ArcGIS was used to create proximity layers for drainage patterns, lineaments, and roadways. The Geological map of Jammu and Kashmir by Thakur and Rawat (1992) was employed to generate a geology map of the study region. After assessing the average annual gridded rainfall data (1990-2021) from the Indian Metrological Department (IMD), we converted the gridded rainfall data into point data and used an interpolation approach to construct a final rainfall map of the study area in ArcGIS. Likewise, steps like LSZ's projections, digitization, thematic map creation, and thematic map integration were accomplished in ArcGIS 10.8. All the Thematic layers were converted to raster format using 15×15 m grid cells in a UTM Projection; Zone 43; Datum WGS 84 (Tian et al. 2008). Table 2 shows the datasets and sources used in the current study. The study's overall Methodological approach is depicted in Fig. 2.

Landslide Causative Factors

Slope gradient

The steepness of the slope is a basic factor in determining the landslide frequency of any region. It is a crucial element in landslide incidence (Donnarumma et al. 2013). The steep angle of the slope causes the material to become unstable. Likewise, slope stability is instantly impacted due to the change in shear forces of the material (Lee and Min. 2001). The slope gradient also affects water flow (Pourghasemi et al. 2012). Using the Jenks natural breaks categorization method, the slope gradient map (Fig.5a) was divided into seven (7) groups (Jenks. 1967): 5 (Gentle Slope), 5–8.5 (Moderate Slope), 8.5–16.5 (Strong Slope), 16.5–24 (Very Strong Slope), 24–35 (Extreme Slope), 35–45 (Steep Slope), and >45 (Very Steep Slope).

Slope aspect

The slope's aspect shows which orientation it is sloping. Aspect influences water flow, erosion characteristics, and solar exposure (Singh and Kumar. 2018). In the present study, the slope aspect was extracted from ALOS Dem and

was reclassified into nine (9) distinct groups (Jenks. 1967), viz; North, Northeast, East, Southeast, South, Southwest, West, Northwest, and Flat (Fig.5b). Moreover, slopes towards South, North, and South-west are where most of the landslide regions are located.

Curvature

The definition of curvature is the slope of a slope. Specifically, this is a second surface derivative. A positive curvature value suggests a convex surface, whereas a negative value denotes a concave surface. A 'zero' represents a perfectly flat surface. Curvature infers the influence of water in landslide hazard zones (Ohlmacher. 2007). This study generated a curvature from ALOS Dem in ArcGIS 10.8 and classified it into three groups (Fig. 5d): concave (-0.639999986), flat (-0.639999986-0), and convex (0 - 43.13851027).

Elevation

A key indicator of landslide risk is the elevation of the terrain. The ASTER Dem was used to extract and produce an elevation map. As landslides frequently occur at higher elevations, earthquakes are also significantly influenced by height. In the area under study, elevations vary from 1,098 to 3,475 meters. In this study, the elevation map was reclassified into five groups (Jenks 1967): 1,098 - 1,627 m, 1,627 - 1,903 m, 1,903 - 2,202 m, and 2,202 - 2,579 m (Fig.5c).

Proximity to Drainage

Rivers are significant in developing landslides (Park et al. 2013). Furthermore, due to slope sub-quotation, and gully erosion, these can destroy banks and shifting terrain, affecting landslide initiation (Bui et al. 2011). The drainage network of the research area was created from ALOS Dem by using hydrology tool of ArcGIS. In the present study, we generated five distinct buffer groups in the present investigation, including 0-150, 150-300, 300-450, 450-600, and >600 m (Fig.5g).

Proximity to Lineaments

The relatively straight alignments of linear or curvilinear patterns in satellite imagery indicate the presence of lineament, which is composed of structurally regulated linear or curvilinear structures. These details reveal the surface topography beneath the structural details. Many landslides are triggered by lineaments, which are caused by tectonic fractures that typically reduce rock strength and are also required for susceptibility studies. In the current study, lineaments were digitized using high-resolution imageries and backed up by lineament data from the NRSC Bhuwan. Finally, the study area was divided into five distinct buffer zones in ArcGIS 10.8 (Fig.5h). viz., 0-500, 500-1000, 1000-1500, 1500-2000, and >2000 m.

Proximity to Roads

Another key aspect in affecting the likelihood of landslides is their proximity to roads. The cutting activities involved in road construction alter the terrain's natural slopes (Siddique et al. 2017). As a result, the slope at the toe weakens along the roadways. The roads were digitized manually from the SOI toposheets and updated with the high-resolution Google Earth Imageries. Furthermore, the study region was categorized into five buffer groups viz: 0-500, 500-1500, 1500-2500, and >2000 m (Fig. 5i).

Rainfall

Increased Pore-water pressures in the ground typically cause rain-induced landslides (Sati. 2014). Rainfall, which is believed to be a trigger for the onset of landslides, is among the most critical elements in landslide susceptibility assessment. For this study, Long Period Average (LPA) yearly IMD rainfall data was used to develop a rainfall map. Further, this resultant map was reclassified into three groups (Fig. 5j): Low (1,014 -1,093), Moderate (1,093 -1,144), and High (1,144 - 1,193) mm/yr.

Land use/Land cover

Slope stability is greatly influenced by land use and land cover (Ocakoglu et al. 2002). Human needs are a driving force behind many land use shifts, including converting rural and forested areas into urban centers, cultivating forestry land, and leveling slopes to improve infrastructure development. Compared to areas with little or no vegetation, those with thick vegetation are less likely to experience landslides (Gokceoglu and Aksoy 1996). Due to the accelerated expansion of infrastructure and development projects in steep locations, the slope is becoming more and more susceptible to landslides. For this study, bare ground is considered highly landslide-prone. In this study, lulc was reclassified into eight categories (Fig.5f), viz., Settlement (Mixed built-up) (4.42%), Barren land (21.10%), Agriculture (16.65%), Dense Forest (29.63%), Scrub/Shrub (4.19%), Sparse Forest (22.58%), Pastures (0.01%) and Waterbodies (1.42%)

Geology

The primary use of the geological map of an area is for assessing landslide hazards (Thennavan and Pattukandan Ganapathy 2020). So different geological units are important for analyzing vulnerable zones due to their varying landslide sensitivity levels. In the present study, the geological map was generated from the geological map of Jammu and Kashmir by Thakur and Rawat (1992) and reclassified into ten categories. The spatial distribution of various geology types in the study region is depicted in Fig.5e. The Salkhala Formation, Upper Triassic Limestones, Panjal Volcanics, Thrust, Murree/Dharamshala, Pampur member (Karewa formation), Alluvium, Basement Inliers (Permian-Triassic), Dilpur Formation (Karewa formation), and Hirpur Formation (Karewa formation) are among the ten geological features in the study. According to the AHP analysis, Upper Triassic limestones have the highest proportion (41.27 %), followed by the Salkhala formation (28.57 %) and Alluvium (11.11 %) of landslide occurrences. The geology types, Murree/Dharamshala, Pampur member, and Dilpur Formation classes, possess no landslide occurrences. Landslides are influenced by alluvium and limestone deposits because of their strong capacity to absorb water. Due to their weak water adsorption capacity and semi-permeability, gneiss and states-schist are geological blocks that are somewhat prone to landslides.

Landslide Susceptibility Zonation (LSZ) Mapping

Assignment of weights and normalization of weights using AHP

Since the findings of the integrated analysis are highly sensitive to the weights allocated to the various classes, this step is of utmost importance (Kayastha et al. 2013). Due to its capacity to produce fast, accurate, and cost-effective results, the AHP is gaining interest in landslide prediction modeling. AHP is a pairwise matrix analytical method used to get a single parameter's geometric mean and normalized weight (Saaty and Vargas 1980). In landslide hazard

analysis, the AHP technique establishes a hierarchy of criteria for problem-solving by first outlining the research objectives and then specifying the criteria and sub-criteria to evaluate those objectives. Several studies have utilized the AHP to rank the significance of different criteria and sub-criteria (Myronidis et al. 2016; Kayastha et al. 2012; Thanh and de Smedt 2012; and Yalcin et al. 2011). On basic Saaty's 1-9 scale, where "1" means "equal importance," we assigned relative significant values to all data layers(themes) and their corresponding attributes. In Table 3, "9" indicates "great significance" for one theme over another (Saaty and Vargas 1980). Likewise, in Table 4, the Random Inconsistency (R.I) value is listed for the corresponding number of Criteria (Saaty 1987). Besides, Table 5 displays the relative importance among various classes and their corresponding class types(attributes).

Therefore, the final thematic layer weights were determined by the following steps.

1. Using the formula, we added the numbers in each column of the pairwise matrix (Table 6).

$$L_j = \sum_{ij=1}^{n} C_{ij} \quad \textbf{(1)}$$

Lj = sum of each pairwise matrix column's values and Cij = The Number at the ith row, jth column that corresponds to each criterion.

2. A normalized pairwise matrix is obtained by dividing each matrix entry by the sum of each column (Table 7).

$$X_{ij} = \frac{C_{ij}}{L_j} \quad \textbf{(2)}$$

Xij = Normalized pairwise matrix values for the ith row and jth column.

3. When determining standard weights, the normalized row matrix sum is divided to the total number of criteria used (N).

$$\mathrm{W}_i = \frac{\sum X_{ij}}{N} \quad \textbf{(3)}$$

Where Wi = Standard weight.

4. Analysing for Consistency.

Multiplying each thematic layer's pairwise comparison matrix with its normalized pairwise comparison matrix yields the consistency vector. Likewise, the values of the consistency vector were entered into the following equation:

$$\lambda = \sum C_{ij} X_{ij} \quad \textbf{(4)}$$

where λ = Consistency vector.

5. One more appealing point for the AHP is its ability to assess disagreement in ratings between pairs. A consistency measure that indicates inconsistencies in a given set of pairwise ratings can be quantified using the eigen values. For instance, Saaty (2000) showed that the maximum eigenvalue 'λMax' for a consistent reciprocal matrix is equal to the number of comparisons. Hence,the consistency index (CI) is a measure of consistency and is defined as follows:

$$CI = \frac{\lambda \max - n}{n-1} \quad \textbf{(5)}$$

Where, “CI” and “n” correspond to Consistency Index value and the Number of criteria utilized respectively for the study.

6. The C.R. introduced by Saaty (1977) compares the values of the consistency index with the random consistency index (Table 8). The formula to determine the consistency ratio (CR) is given below.

$$CR = \frac{CI}{RI} \quad \textbf{(6)}$$

Where, “RI” denotes the Random Inconsistency value (also known as Randomized index of Saaty, 1990)

Furthermore, we can accept inconsistency if the ratio is below 10%. If not, we'll adjust the subjective assessment (Saaty 1977). Moreover, the values of RI for a set of ‘n’ criteria, where ‘n’ denotes the entire number of criteria utilized, as given in Table 4.

Assessment of Landslide Susceptibility Zonation (LSZ) Map

The LSI measures the potential for landslides and is a dimensionless quantity. Therefore, we located potential landslide areas using a GIS-based MCDA technique. By multiplying the thematic layers' weights with the sub-parameter weights for each layer, we obtained the products of all the characteristics, which then were summed using the formula in eq. 7.

$$LSI = AW\sum_{A=1}^{9} AR + GW\sum_{G=1}^{9} GR + EW\sum_{E=1}^{4} ER + SW\sum_{S=1}^{5} SR + LW\sum_{L=1}^{5} LR + DW\sum_{D=1}^{5} DR + LUW\sum_{LU=1}^{9} LUR + CW\sum_{N=1}^{3} CR + RW\sum_{N=1}^{3} RR + RFW\sum_{N=1}^{3} RFR \quad \textbf{(7)}$$

Where LSI = Landslide susceptibility index; A.W, G.W, E.W, S.W, L.W, D.W, LUW, C.W, R.W, and RFW indicate the corresponding weights of slope aspect, geology, elevation, slope gradient, distance to lineament, distance to Drainage, land use and land cover, curvature, distance to roads, and Rainfall respectively. While as, A.R, GR, E.R, S.R, L.R, D.R, LUR, C.R, R.R, and RFR represent the assigned weights of each parameter sub-class, namely aspect, geology, elevation, slope gradient, lineament, Drainage, land use and land cover, curvature, roads, and Rainfall respectively. Therefore, AHP provides a comprehensive criterion ranking method by applying the comparison matrix among all options and data on criterion ranking. Furthermore, the most essential element is the one with the highest value.

Results and discussion

In the current research work, ten potential causative factors have been investigated in the study region using the MCDA (AHP) technique, and accordingly, thematic layers have been created in the GIS platform. After that, we assigned a weight to numerous elements inside each thematic layer by landslide type and location. Based on expert opinion, values between 1 (equal) and 9 (highest) have been assigned to each set of parameters. Class and class features within each factor are depicted in Table 5, while as, pairwise comparisons of the causal factors are shown in Table 6, with the degree of the slope being given the highest weight. Also, Table 6 displays both the lower part of the matrix

values and the reciprocal upper part of the matrix. The normalized principal eigenvector is tabulated in the final column of the matrix. For example, the slope receives the most significant weight of 0.257, and LULC receives the least weight of 0.020. The sum of the allocated weights equals to one. The consistency ratio is checked against the ratings and weights before index values are calculated using Equation 5 for the calculation of CI and Equation 6 for the calculation of C.R. Hence, C.R. Scores below 0.10 in (Table 8) show that the preferences used to generate the comparison matrix are stable. Finally, a hazard zonation map for the area was generated using the GIS-based MCDA (AHP) approach with the help of the given weighting values (Fig.5). The AHP-generated LSZ map was then divided into five hazard classes (Table 8), using the Jenks natural breaks categorization system: very high (24.18%), high (30.24%), moderate (28.61%), low (15.28%), and very low (1.69%). Also, Fig 7 displays the percentage of each categorized class's area.

The LSI map was prepared, categorized, and validated by using the natural break method (Jenks 1967) in GIS platform. The proportion of landslides found in each class of the final map was computed by combining the reclassified susceptibility zonation map with the landslide inventory dataset using a tabular tool in ArcGIS. The predictive accuracy of the AHP model for the current study was found to be 79.8%. Moreover, a detailed landslide field investigation was conducted in the research area (Fig.9). During the validation process, it was observed that the LSZ map and pre-existing landslide location datasets are showing a high level of satisfactory agreement. Therefore, study suggests that almost all landslide locations fall under the high and very high susceptible categories. Thus, the AHP method and phenomena are a perfect match for the real situations in the current study region. However, the map's reliability depends on the data collection's precision, method's robustness, and the landslide prediction experience.

Very high susceptible zone

A total of 116.02 km^2 (24.18%) studied area lies under very high landslide susceptibility zone (Fig. 7 & Table 8). Moderate to very high steep slopes, Triassic limestone, Salkhala formation, Muree formation, settlement, barren land, proximity to drainage, lineament, road mostly 5oom, low to mid-elevations, south, southwest, North aspects are the characteristics of this class. Most settlements between Baramulla to Uri Road stretch fall within this category, particularly Uri reservoir, Chollan Kalsan, and Limber.

High susceptible zone

The high susceptibility zone encompasses 145.12 Km^2 of the area accounting 30.24 % of the whole research area (Table 8). It is characterized by steep slopes, high elevations, predominantly salkhala, Upper Triassic limestones, Panjal volcanics, and Alluvium formations. Furthermore, this zone largely lies in a moderate to high precipitation region which encompasses the Barrren land, scrubs, sparse forests, and settlements. The proximity to roads, lineaments, and rivers/streams is extremely minimal in most of this zone. The villages falling under this category are Uri, Boniyar, Lagama, Nalusah, Bimyar, Kitchama and Sheeri.

Moderate susceptible zone

A total of 136.2 km^2 (28.61 percent) research area falls within the moderate susceptibility zone (Table 8), primarily on the Scrubs, sparse forests, Pastures, and Agriculture land use classes. This zone is further distinguished by its moderate to strong slopes, sandy skeletal soil, and exceptionally moderate to low precipitation region. Besides, this class is dominated by Salkhala, Alluvium, Hirpur and Dilpur geological formations. Furthermore, this zone resides a small valley with high and low altitudes, moderate slope classes, and the area at less proximity to rivers and faults. Moreover, the villages falling under this hazard category are Pahlipora and Khadaniar.

Low and very low susceptible zone

In the current study, these susceptible zones account for 16.97% of the 864.84 km^2 study area (Table 8). Likewise, these zones are particularly prevalent on gentle-moderate slopes with exceptionally steep slope classes. Further, these zones are situated at a substantial distance from roads, lineaments, and rivers on Salkhala, Dilpur, Hirpur and Alluvium geological formations predominantly. The villages falling under these classes are Baramulla, Gantmulla payeen, Khanpora and Janbaz colony.

Accuracy Assessment of LSZ map

For LSZ map's validation, the ROC is a frequently used method (Roy and Saha. 2019). In addition, this method evaluates the accuracy of a generated LSZ map and calculates its ability to predict in terms of AUC value. Likewise, the True Positive Rate (TPR) versus the False Positive Rate (FPR) is often illustrated graphically utilizing ROC curves (Althouse. 2016). Furthermore, the specificity and sensitivity values are used to construct the AUC curve to describe model performance, with a value closer to 1 indicating exceptional goodness of fit and an AUC value less than 0.5 indicating that the model precision level is unsatisfactorily low (Pradhan and Kim 2016).

The final resultant map in the study region was validated by superimposing data from 30 percent of the landslide locations, previously designated as testing samples. For this purpose, 30% of total landslide points were collected using a GPS device during a field survey and compared with the final LSZ map depicting five levels of susceptibility. Besides, AUC value calculation was the prime criteria for precisely evaluating the model (Fig.8). Therefore, from the ROC curve, the AHP-generated LSZ map (with an AUC value of 79.8%, which is good) is quite accurate in terms of landslide prediction.

From the past two decades, numerous approaches for mapping landslide risk have been developed including qualitative, semiquantitative, and quantitative methods. None of these approaches, however, are generally accepted for use in assessing the risk of landslides due to ongoing arguments regarding their accuracy. Consequently, for the current study, a GIS-based multicriteria decision-making method was utilized to determine the most probable landslide events. This method examines multiple landslide causal factors, although it may be hard to quantify their contributions. This study employed an AHP method to assign relative relevance weights to landslide-triggering causal factors. Likewise, a knowledge-driven expert opinion was employed for the pairwise comparison of the causative factors to establish consistent and trustworthy weights. Subsequently, the multicriteria criteria evaluation (MCE) analysis was applied for the LSI calculation of final LSZ map. The spatial efficiency of the resultant LSZ map assessed by AUC

shows that the used model performed well (with an overall accuracy of 79.8 %). The AHP model is adaptive and produces good results, although causation with respect to landslide inventory in our research region is unclear. Likewise, availability of large-scales geological maps, high-resolution satellite imageries and digital elevation models (DEMs), and landslide data is scarce, limiting this study's landslide and time parameter/factor selection. Hence, AHP was chosen due to inadequate NH-1 landslide data and its suitability for large-scale assessments or places without inventory (Zhou et al. 2016).

Planning and control of landslide hazards could be improved with the help of the study's LSZ map. The resultant LSZ map might be used to recognize high-vulnerable areas and emphasize the installation of early warning systems and other preventative measures like increased vegetation cover, improved drainage, slope stabilization, and so on. The LSZ map can serve as a reference for transportation, and structural planning in the study region, with the goal of potentially reduce the effects of landslides.

Moreover, there are certain limitations to the study that should be considered. Since the study only reflected ten potential causal factors, additional elements including rock characteristics, soil parameters, and seismicity were not encompassed. Likewise, the study did not include the temporal variations of the causal parameters that could alter the landslide-susceptible zones, which is another limitation of the research. In addition to primary data sources, this study made use of some ancillary (secondary database) databases, which may have some limitations in spatial resolution and accuracy.

Conclusion

This research focuses on a section of the NH-1 highway which is frequently impacted by landslide disasters. Planning and executing highway building projects necessitate a landslide hazard assessment. In the present work, a LSZ map was prepared using Geospatial tools and the AHP (Saaty and Vargas 1980) model along NH-1 in the Kashmir Himalaya, India. Ten important causal parameters of landslide occurrences were considered for the thematic data layer generation in a GIS platform. On Saaty's scale, suitable weights were assigned to the ten selected thematic maps and their characteristics based on their relative importance in AHP. Subsequently, AHP was applied to normalize the weights given to various GIS data layers(themes) and their corresponding classes. The LSI was estimated using weighted linear technique and finally LS maps were produced in a GIS. Later, LSZ map of study area was reclassified into five distinct susceptible classes viz; very high, high, moderate, low, and very low susceptible zones.

According to the landslides susceptibility Assessment (LSA), most of the study region (54.42 %) constitutes very high and high vulnerable zones due to lineaments (thrusts, faults, joints), steep slopes, improper drainage system, road widening, and weak lithology. As a result, regions near lineaments, drainage, roadways, and steep slopes are most vulnerable to landslides and hence highly unsafe for construction purposes. Likewise, areas that are composed of weak Triassic limestones and alluvium geological formations are highly insecure for construction purposes. These findings suggest that Limber, Chollan kalsan, Uri, sheeeri, boniyar, lagama, and Khadaniar are unsafe and highly prone to landslides in the future. In addition, 44% of the research area was classified as a low or moderately susceptible zone.

From the study analysis, it is safe to build in low vulnerable zones; nevertheless, moderately vulnerable zones require extensive geotechnical investigation prior to any future development.

The final LSZ map was validated using the ROC curve approach. The validation data revealed that the AHP method has a greater prediction accuracy (78.9 %). Therefore, the produced LSZ map is valid for landslide assessment, risk evaluation, mitigation measures, and for any future developmental projects in the region. Furthermore, it will provide the public, engineers, and planners with enough knowledge about the present and future likelihood of landslides to mitigate construction hazards for high / very high-risk zones.

Acknowledgment

The authors would like to express their gratitude to the Geological Survey of India (GSI) and the Border Roads Organization (BRO) in Srinagar, Jammu and Kashmir, India, for supplying the necessary landslide data. In addition, the authors would like to express their gratitude to everyone who assisted them, while conducting the fieldwork. In addition, the authors would like to use this opportunity to extend their heartfelt appreciation to the Department of Civil Engineering at the National Institute of Technology (NIT) in Srinagar, Jammu and Kashmir, India, for making the essential research facilities available. In addition, the authors would like to express their sincere gratitude to the reviewers for their insightful remarks and recommendations.

Compliance with ethical standards

Conflict of interest. The corresponding author declares that there is no conflict of interest on behalf of all authors.

References

Abhijit, S.P., Bidyut, B. K., Sachin P.S & Sudhir, P.K. (2021). The Landslide Susceptibility Assessment using Bi-variate Statistical Information Value Model of Chenab River Valley, Jammu and Kashmir (India). *Disaster Advances, 14*(11), 44-56. https://DOI: 10.25303/1411da4456

Agarwal, D.K., Krishna, A.P., Joshi, V., Kumar, K & Palni, L.M.S. (1997). Perspectives of Mountain Risk Engineering in the Himalayan Region. Himavikas Occasional Publication No. 10, G.B. Pant Institute of Himalayan Environment and Development, Almora (India), Gyanodaya Prakashan, Nainital, India. 244.

Aleotti, P., Chowdhury, R. (1999). Landslide hazard assessment: summary review and new perspectives. *Bulletin of Engineering Geology and the Environment*, *58*(1), 21-44.

Althouse, A.D. (2016). Statistical graphics in action: making better sense of the ROC curve. *Int. J. Cardiol,* 215, 9–10. https://doi.org/10.1016/j.ijcard.2016.04.026.

Balew, A., Alemu, M., Leul, Y., & Feye, T. (2020). Suitable landfill site selection using GIS-based multi-criteria decision analysis and evaluation in Robe town Ethiopia.*GeoJournal,87*,895–920. https://doi.org/10.1007/s10708-020-10284-3.

Bashir, S., & Ramkumar, T. (2021). A multi-temporal landslide inventory and hazard zonation using relative effect method along the Mughal Road Shopian, India. *Disaster Advances*, *14*(7), 42. http://dx. doi.org/10.25303/147da4221

Bathrellos, G.D., Gaki-Papanastassiou, K., Skilodimou, H.D., Papanastassiou, D., Chousianitis, K.G. (2012). Potential suitability for urban planning and industry development using natural hazard maps and geological–geomorphological parameters. *Environ. Earth Sci.,* 66, 537–548.

Bilham, R., Bali, B.S. (2014). A ninth-century earthquake-induced landslide and food in the Kashmir Valley and earthquake damage to Kashmir's Medieval temples. *Bull Earthq*, *12*(1), 79–109.

Bui, D.T., Lofman, O., Revhaug, I., & Dick, O. (2011). Landslide susceptibility analysis in the Hoa Binh province of Vietnam using statistical index and logistic regression. *Natural Hazards, 59*, 1413.

Castellanos Abella, E. A. (2008). Multi-scale landslide risk assessment in Cuba. ITC.

Chaiyaphan, C., Ransikarbum, K., Sriariyanun, M., Cheng, Y.S., Rattanaporn, K., Yasurin, P., et al. (2020). Criteria Analysis of Food Safety using the Analytic Hierarchy Process (AHP) - A Case study of Thailand's Fresh Markets. *E3S Web Conferences*; *141*, 02001. doi: https://doi.org/10.1051/e3sconf/ 202014102001.

Chen, Z.; Zhang, B.; Han, Y.; Zuo, Z.; Zhang, X. (2014). Modeling accumulated volume of landslides using remote sensing and DTM data. Remote Sens., 6, 1514–1537.

Chingkhei, R.K., Shiroyleima, A., Robert Singh., L, & Kumar, A. (2013). Landslide Hazard zonation in NH-1A in Kashmir Himalaya,India. *InternationalJournal of Geosciences*, *4*,1501-1508.http://dx.doi.org/10.4236/ijg.2013.410147

Cruden, D., VanDine, D.F. (2013). Classification, Description, Causes and Indirect Effects—Canadian Technical Guidelines and Best Practices Related to Landslides: A National Initiative for Loss Reduction; Geological Survey of Canada, Open File 7359; Natural Resources Canada: Ottawa, ON, Canada.

Cruden, D.M. (1991). A simple definition of a landslide. *Bulletin of the International Association of Engineering Geology*, *43* (1), 27- 29.

Cruden, D.M., Varnes, D.J. (1996). Landslide types and processes. In Landslides, Investigation and Mitigation, 1st ed.; Turner, A.K., Schuster, R.L., Eds.; Transportation Research Board: Washington, DC, USA, 36–75.

Dagdelenler, G., Nefeslioglu, H. A., & Gokceoglu, C. (2016). Modification of seed cell sampling strategy for landslide susceptibility mapping: an application from the Eastern part of the Gallipoli Peninsula (Canakkale, Turkey). *Bulletin of Engineering Geology and the Environment*, *75*(2), 575-590.

Dikshit, A., Sarkar, R., Pradhan, B., Segoni, S., & Alamri, A.M. (2020). Rainfall induced landslide studies in Indian Himalayan region: a critical review. *Appl Sci, 10* (7), 2466. https://doi.org/10.3390/app10072466

Donnarumma A., Revellino P., Grelle, G., & Guadagno, F.M. (2013). Slope angle as indicator parameter of landslide susceptibility in a geologically complex area. In: Margottini C, Canuti P, Sassa K, editors. Landslide Science and Practice. Berlin, Heidelberg: Springer; 425–33. doi: https://doi.org/10.1007/978-3- 642-31325-7_56.

Fan, W., Wei, X., Cao, Y., & Zheng, B. (2017). Landslide susceptibility assessment using the certainty factor and analytic hierarchy process. *J Mountain Sci*, *14* (5), 906–25. doi: https://doi.org/10.1007/s11629-016-4068-2.

Fell, R., Corominas, J., Bonnard, C., Cascini, L., Leroi, E., & Savage, W. Z. (2008). Guidelines for landslide susceptibility, hazard and risk zoning for land-use planning. *Engineering geology*, *102*(3-4), 99-111.

Gokceoglu, C., & Aksoy, H. (1996). Landslide susceptibility mapping of the slopes in the residual soils of the Mengen region (Turkey) by deterministic stability analyses and image processing techniques. *Engineering Geology. 44* (4), 147-161.

Guzzetti, F., Carrara, A., Cardinalli, M., & Reichenbach, P. (1999). Landslide hazard evaluation: a review of current techniques and their application in a multi-case study, Central Italy. *Geomorphology*, *31*(1–4):181–216.

Hussain, G., Singh, Y., & Bhat, G.M. (2015). Geotechnical investigation of slopes along the National Highway (NH-1D) from Kargil to Leh, Jammu and Kashmir (India). *Transport Res Rec*, *5*, 56–67.

Hussain, G., Yudhbir, S., Ghulam, M.B. (2018). Landslide susceptibility mapping along the National Highway 1D, between Kargil and Lamayuru, Ladakh Region, Jammu and Kashmir. *Geol Soc India 91*, 457–466.

Jamir I, Gupta V, Thong GT, Kumar V. (2019). Litho-tectonic and precipitation implications on landslides, Yamuna valley, N.W. Himalaya. Phys Geogr 41:1–24. https://doi.org/10.1080/02723646. 2019.1672024

Jenks, G.F. (1967). The data model concept in statistical mapping. *Int Year b Cartography 7,* 186–190.

Kamp, U., Growley. B.J., Khattak, G.A., & Owen, L.A. (2008). GIS-based landslide susceptibility mapping for the 2005 Kashmir earthquake region. *Geomorphology, 101*(4), 631–642.

Kayastha, P., Dhital, M.R., & De Smedt, F. (2013). Application of the analytical hierarchy process (AHP) for landslide susceptibility mapping: a case study from the Tinau watershed, west Nepal. *Compu. Geosci*., 52, 398–408. https://doi.org/10.1016/j. cageo.2012.11.003.

Kayastha, P., Dhital, M.R., Smedt, F.D. (2012). Application of the analytical hierarchy process (AHP) for landslide susceptibility mapping: A case study from the Tinau watershed, West Nepal. *Computers Geosci.*, *52*, 398–408. doi: https://doi.org/10.1016/j.cageo.2012.11.003.

Keefer, D.K. (1984). Landslides caused by earthquakes. *Geological Society of America Bulletin*, *95*(4), 406-421.

Khattak, G.A., Owen, L.A., Kamp, U., & Harp, E.L. (2010). Evolution of earthquake-triggered landslides in the Kashmir Himalaya northern Pakistan. *Geomorphology*, *115*(12), 102–108.

Kumar, R., Anbalagan, R., 2016. Landslide susceptibility mapping using analytical hierarchy process (AHP) in Tehri reservoir rim region, Uttarakhand. J. Geol. Soc. India 87, 271286. Kumar, R., Anbalagan, R., 2015. L

Lageson, D.R., Fort, M., Bhattarai, R.R., Hubbard, M. (2016). Damage from the April–May 2015 Gorkha Earthquake Sequence in the Solukhumbu District (Everest Region), Nepal; GSA Annual Meeting: Denver, CO, USA.

Lee, S., & Min, K. (2001). Statistical analysis of landslide susceptibility at Yongin. Korea. *Environ Geol*, *40* (9), 1095–113. doi: https://doi.org/10.1007/ s002540100310.

Mathew, J., Jha, V.K., Rawat, G.S. (2009). Landslide susceptibility zonation mapping and its validation in part of Garhwal Lesser Himalaya, India, using binary logistic regression analysis and receiver operating characteristic curve method. *Landslides*, *6*, 17–26.

Mohammady, M., Pourghasemi, H.R, Pradhan, B. (2012). Landslide susceptibility mapping at Golestan Province, Iran: a comparison between frequency ratio Dempster-Shafer and weights-of-evidence models. *J of Asian Earth Sci*, *61*, 221–236.

Mohebbi, M., Shakeri, K., Ghanbarpour, Y., & Majzoub, H. (2013). Designing optimal multiple tuned mass dampersusing genetic algorithms (GAs) for mitigating the seismic response of structures. *Journal of Vibration Control*, *19*(4), 605–625.

Mohsin F., Gowhar, M., Khader, S. A., Farooq, M., Kanga, S., Singh, S. K., Kumar, P., & Sahu, N. (2022). Management of Landslides in a Rural–Urban Transition Zone Using Machine Learning Algorithms—A Case Study of a National Highway (NH-44), India, in the Rugged Himalayan Terrains. *Land*, *11*, 884. https://doi.org/10.3390/ land11060884.

Myronidis, D., Papageorgiou, C., & Theophanous, S. (2016). Landslide susceptibility mapping based on landslide history and analytic hierarchy process (AHP). *Natural Hazards*, 81(1), 245–263. https://doi.org/10.1007/s11069-015-2075-1

Nanda AM, Yousuf M, Zahoor ul Islam, Ahmed P and Kanth TA. (2020b). Slope Stability Analysis along N.H. 1D from Sonamarg to Kargil, J&K, India: Implications for Landslide Risk Reduction. *Journal of the Geological Society of India* , *96*,499–506**.**

Nanda, A.M., Hassan, ul Z., Ahmad, P., Kanth, T.A. (2020a). Landslide susceptibility assessment of national highway 1D from Sonamarg to Kargil, Jammu and Kashmir, India using frequency ratio method. *Geo journal 85*(03), 1-14.

National Disaster Management Authority (2009). National Disaster Management Guidelines-Management of landslides and snow avalanches. A publication of the National Disaster Management Authority (NDMA), Government of India, New Delhi.

NRSA, (2001). Atlas on landslide hazard zonation mapping in the Himalayas of Uttarakhand and Himachal Pradesh states using remote sensing and GIS. National Remote Sensing Agency, Hyderabad.

Ocakoglu, F., Gokceoglu, C., Ercanoglu, M. (2002). Dynamics of a complex mass movement triggered by heavy Rainfall: a case study from N.W. Turkey. *Geomorphology*, *42*(3–4), 329–341. https://doi.org/10.1016/ S0169-555X (01)00094-0.

Ohlmacher, G.C. (2007). Plan curvature and landslide probability in regions dominated by earth flows and earth slides. *Eng Geol*, *91*(1–2):117–34. doi: https:// doi.org/10.1016/j.enggeo.2007.01.005.

Owen, L.A., Kamp, U., Ghazanfar, K.A., Harp, E.L., Kefer, D.K., & Bauer, M.A. (2008). Landslides triggered by the 8 October 2005 Kashmir earthquake. Geomorphology, 94, 1–9.

Park, S., Choi, C., Kim, B., & Kim, J. (2013). Landslide susceptibility mapping using frequency ratio, analytic hierarchy process, logistic regression, and artificial neural network methods at the Inje area, Korea. Environmental Earth Sciences 68: 1443–1464.

Pham, B.T., Pradhan, B., Bui, D.T., Prakash, I., & Dholakia, M. (2016). A comparative study of different machine learning methods for landslide susceptibility assessment: a case study of Uttarakhand area (India). *Environ Model Softw., 84*, 240–250.

Pourghasemi, H.R., Pradhan, B., & Gokceoglu, C. (2012). Application of fuzzy logic and analytical hierarchy process (AHP) to landslide susceptibility mapping at Haraz Watershed, Iran. *Nat Hazards, 63*(2), 965– 996. https://doi.org/10.1007/s11069-012-0217-2.

Pradhan, A. M. S., & Kim, Y. T. (2016). Evaluation of a combined spatial multi-criteria evaluation model and deterministic model for landslide susceptibility mapping. CATENA, 140, 125–139. https://doi.org/10.1016/j.catena.2016.01.022

Pradhan, B. (2010). Landslide susceptibility mapping of a catchment area using frequency ratio, fuzzy logic and multivariate logistic regression approaches. *Journal of the Indian Society of Remote Sensing*, *38*(2), 301-320.

Reichnenbach, P., Rossi, M., Malamud, B.D., Mihir, M., & Guzzetti, F. (2018). A review of statistically based landslide susceptibility models. *Earth-Sci Rev*; *180*, 60–91. https://doi.org/10.1016/j.earscirev.2018.03.001.

Roy, J., & Saha, S. (2019). Landslide susceptibility mapping using knowledge driven statistical models in Darjeeling District West Bengal India. Geoenvironmental Disasters, 6(1), 1–18. https://doi.org/10.1186/s40677-019-0126-8.

Saaty, (1987). The analytic hierarchy process-what it is and how it is used. *Mathi Model*, *9* (3–5), 161–176.

Saaty, R.W. (1987). The analytic hierarchy process—what it is and how it is used. *Math Modell*, *9*, 161–76. https://doi.org/10.1016/0270-0255(87)90473-8.

Saaty, T.L. (1977). A scaling method for priorities in hierarchical structures. *J Math Psychol*, *15*(3), 234281

Saaty, T.L. (1980). The analytic hierarchy process. New York: McGraw-Hill.

Saaty, T.L. (2000). Fundamentals of Decision Making and Priority Theory, 2nd ed., RWS Publications.

Saaty, T.L., Vargas, L.G. (1980). Hierarchical analysis of behavior in competition: prediction in chess. *Behav. Sci. 25* (3), 180–191. https://doi.org/10.1002/ bs.3830250303.

Saaty, T. L. (1990). How to make a decision: the analytic hierarchy process. *European Journal of Operational Research*, 48(1), 9–26. https://doi.org/10.1016/0377-2217(90)90057-I

Sangra, R., Singh, Y., Bhat, G.M., Pandita, S.K, & Hussain, G. (2017). Geotechnical investigation on slopes failures along the Mughal Road from Bafiaz to Shopian, Jammu and Kashmir, *India. J Geol Soc, India*, *90*, 616–622.

Sati, V.P. (2014). Towards sustainable livelihoods and ecosystems in mountain regions. Springer International Publishing, pp 137–15.

Shano, L., Raghuvanshi, T.K., & Meten, M. (2020). Landslide susceptibility evaluation and hazard zonation techniques–a review. *Geoenviron-Disasters*, *7* (18), 1–19. https://doi.org/10.1186/s40677-020-00152-0.

Siddique, T., Pradhan, S.P, Vishal, V., Mondal, M.E.A., Singh, T.N. (2017). Stability assessment of Himalayan Road cut slopes along National Highway 58. *India Environ Earth Sci.*, *76*(22). https://doi.org/10.1007/s12665-017-7091-x.

Singh, H., Som, S. (2016). Earthquake triggered landslide – Indian scenario. J Geol Soc India 87(1):105–112. https://doi.org/10.1007/ s12594-016-0378-9.

Singh, K., & Kumar, V. (2018). Hazard assessment of landslide disaster using information value method and analytical hierarchy process in highly tectonic Chamba region in bosom of Himalaya. *J Mountain Sci*, *15*(4), 808–24. https:// doi.org/10.1007/s11629-017-4634-2.

Singh, Y., Sharma, V., Pandita, S.K., Bhat, G.M., Thakur, K.K., & Kotwal, S.S. (2014). Investigation of landslide at Sangaldan near tunnel-47, on Katra Qazigund railway track, Jammu and Kashmir. *J of Geol Soc of India*, *84*(6), 686–692.

Tanyas, H., van Westen, C.J., Persello, C., & Alvioli, M. (2019). Rapid prediction of the magnitude scale of landslide events triggered by an earthquake. *Landslides*, *16*, 661–76. https://doi.org/10.1007/s10346-019-01136-4.

Thanh, L.N., & de Smedt, F. (2012). Application of an analytical hierarchical process approach for landslide susceptibility mapping in A Luoi district, Thua Thien Hue Province, Vietnam. *Environmental Earth Sciences 66* (7), 1739–1752. https://doi. org/10.1007/s12665-011-1397-x.

Thennavan, E., Pattukandan Ganapathy, G. (2020). Evaluation of landslide hazard and its impacts on hilly environment of the Nilgiris District - a geospatial approach. *Geoenviron Disasters 7*(1). https://doi.org/10.1186/s40677-019-0139-3.

Tian, Y., Xia,O. C., Liu, Y., Wu, L. (2008). Effects of raster resolution on landslide susceptibility mapping: a case study of Shenzhen. Sci China Ser E. *Technol Sci*., *51*(2), 188-198.

Varnes, D.J. (1978). Slope movement types and processes. *Spec Rep*, 176:1133.

Xie, X.J., Wei, F.Q., & Zhang, J. (2015). Application of projection pursuit model to landslide risk classification assessment. *Earth Science—Journal of China University of Geosciences*, *40*(9), 1598-1606.

Yalcin A., Reis S., Aydinoglu A.C., Yomralioglu, T. (2011). A GIS-based comparative study of frequency ratio, analytical hierarchy process, bivariate statistics and logistic regression methods for landslide susceptibility mapping in Trabzon, NE Turkey. *CATENA,* 85,274–287

Yang, Z.Y., Pourghasemi, H.R., Lee, Y.H. (2016). Fractal Analysis of Rainfall-Induced Landslide and Debris Flow Spread Distribution in the Chenyulan Creek Basin, Taiwan. *Journal of Earth Science*, *27*(1), 151-159.

Zhou C., Yin K, Cao Y., Ahmed, B. (2016). Application of time series analysis and PSO–SVM model in predicting the Bazimen landslide in the Three Gorges Reservoir, *China. Eng Geol*., 204, 108–120.

Figures

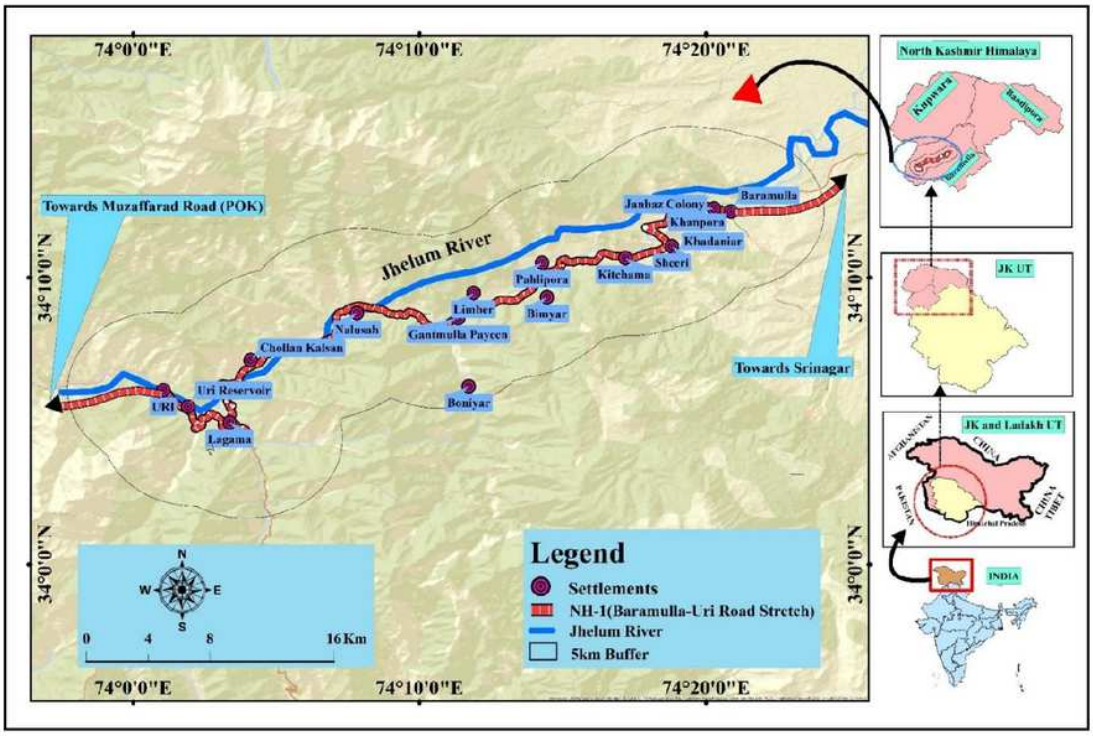

Fig. 1 Location map of Study Area

Figure 1

See image above for figure legend

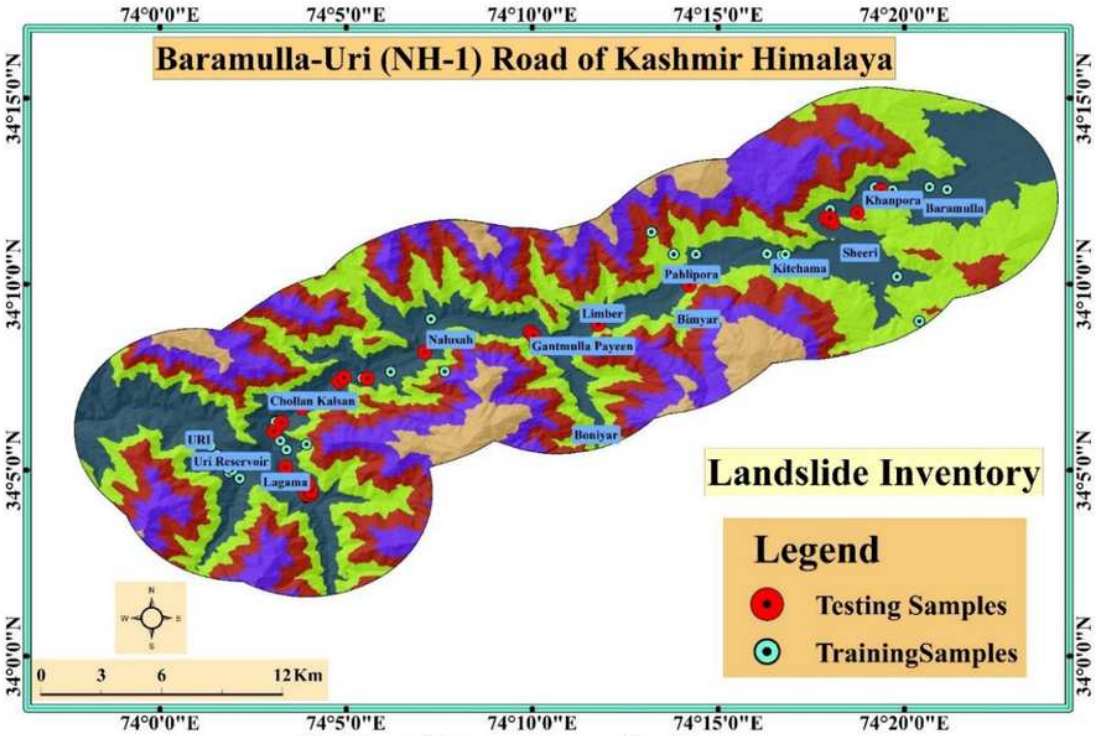

Fig. 2 Landslide Inventory map of the Study Area

Figure 2

See image above for figure legend

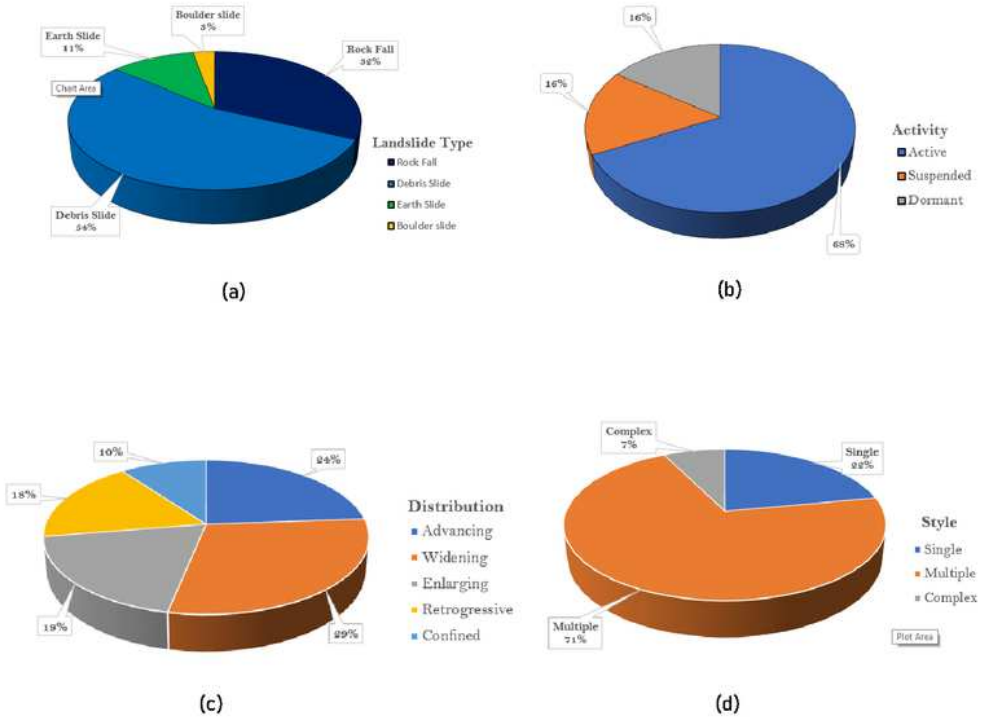

Fig. 3 (a) mode of landslide movement; **(b)** different types of activity;**(c)** distribution of activity; and **(d)** styles of activity in the study area.

Figure 3

See image above for figure legend

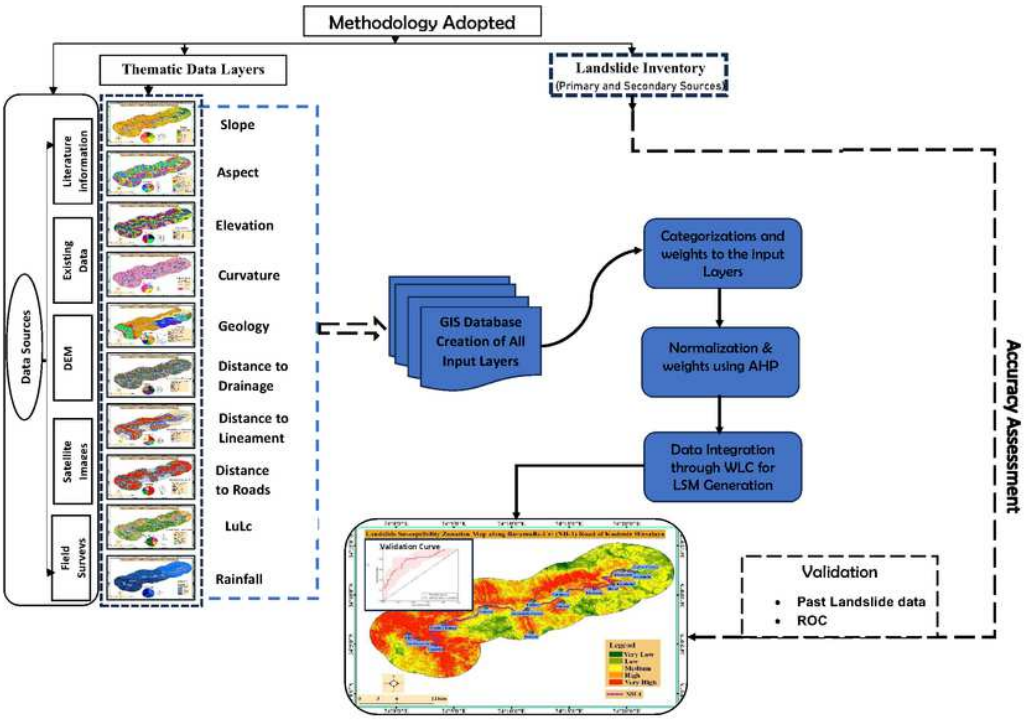

Fig. 4 Flow chart of Landslide Susceptibility Zonation in the Study Area.

Figure 4

See image above for figure legend

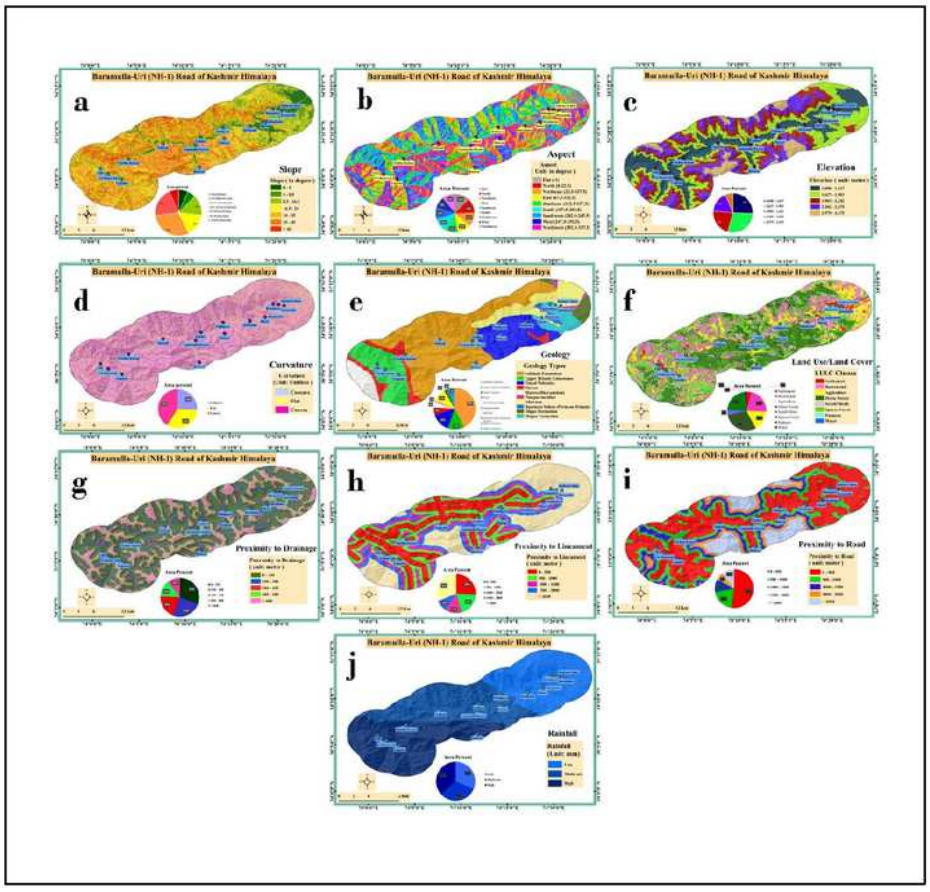

Fig. 5 Landslide Causative parameters used in this study: **a** Slope gradient, **b** Slope aspect, **c** Elevation, **d** Slope Curvature, **e** Geology, **f** Land use Land cover, **g** Proximity to Drainage, **h** Proximity to Lineament, **i** Proximity to Road, **j** Rainfall.

Figure 5

See image above for figure legend

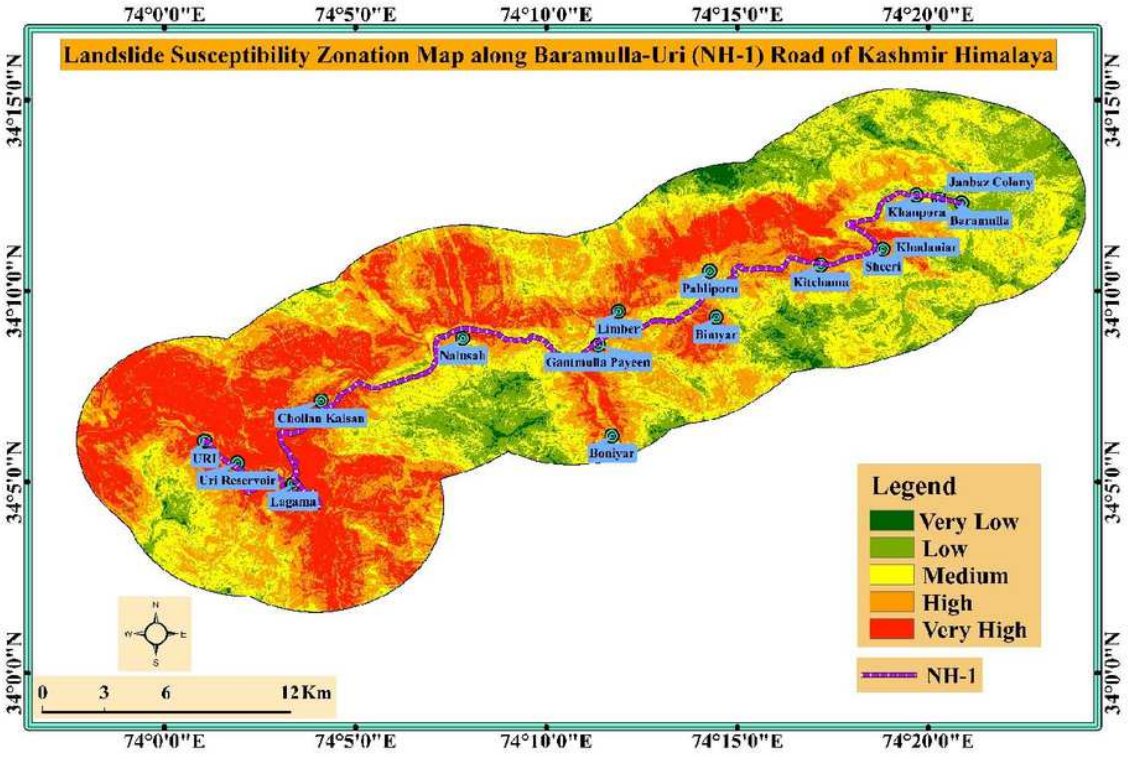

Fig. 6 Landslide Susceptibility zonation map of the study area using Analytical Hierarchical Model.

Figure 6

See image above for figure legend

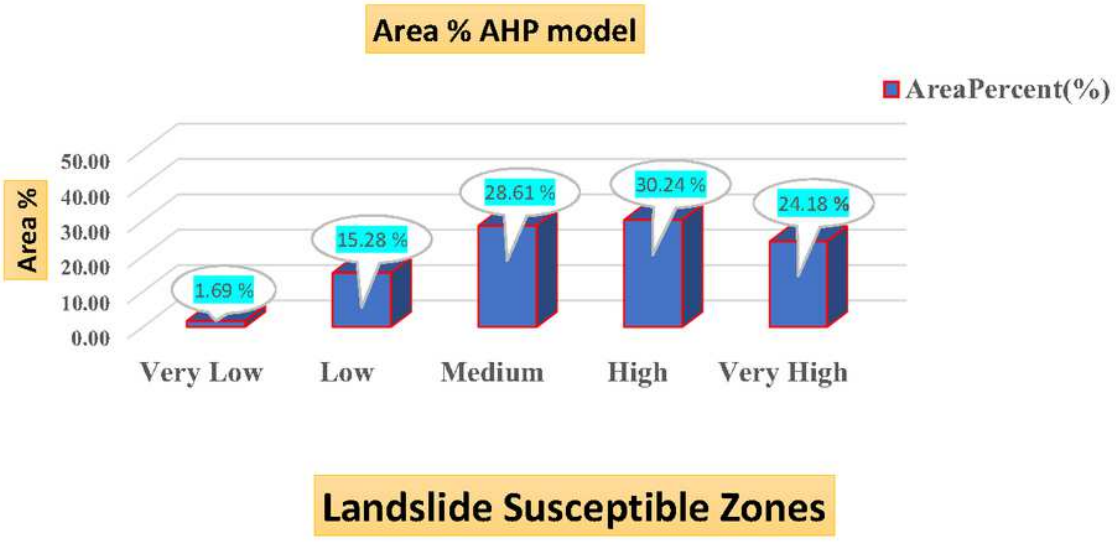

Fig. 7 AHP model-based area of classes on the Landslide Susceptibility zonation map.

Figure 7

See image above for figure legend

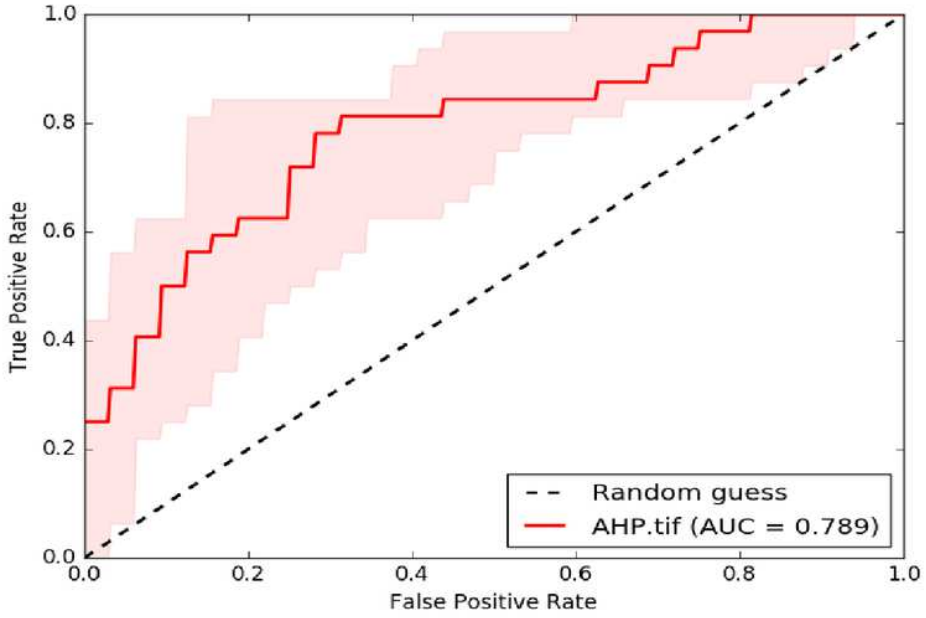

Fig. 8 ROC Curve for landslide susceptibility zonation map validation assessment.

Figure 8

See image above for figure legend

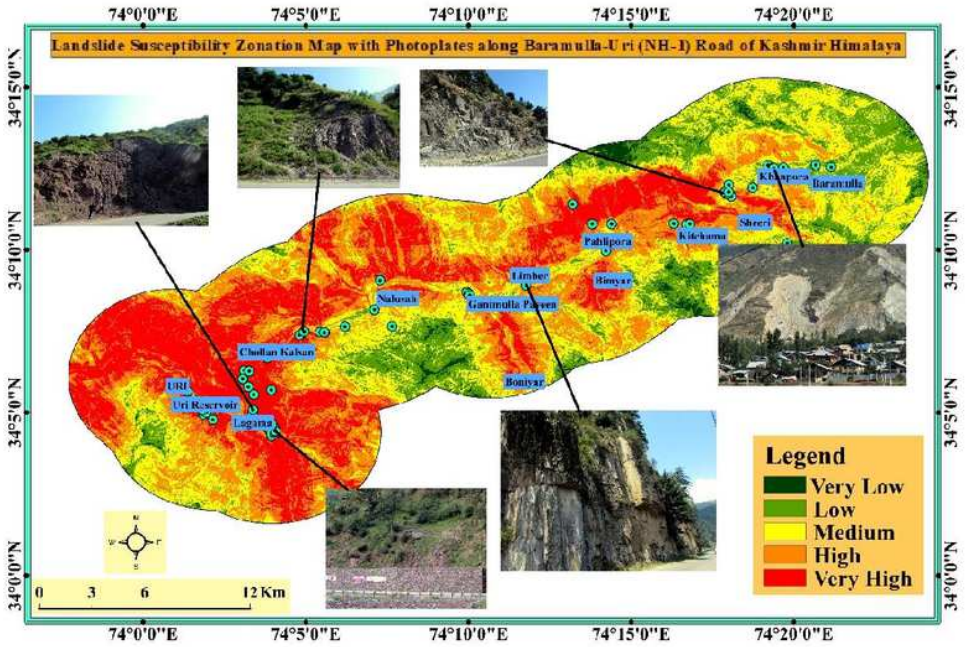

Fig. 9 Photo plates of fieldwork in the study area.

Figure 9

See image above for figure legend

Supplementary Files

This is a list of supplementary files associated with this preprint. Click to download.

- Tables.pdf